2021-09-01

Prodromal dysfunction of a5GABA-A receptor modulated hippocampal ripples occurs prior to neurodegeneration in the TgF344-AD rat model of Alzheimer's disease

Heliyon 7 (2021) e07895

Contents lists available at ScienceDirect

Heliyon

journal homepage: www.cell.com/heliyon

Research article

Prodromal dysfunction of α5GABA-A receptor modulated hippocampal ripples occurs prior to neurodegeneration in the TgF344-AD rat model of Alzheimer's disease

Marcia H. Ratner [a], Scott S. Downing [a], Ouyang Guo [d], KathrynAnn E. Odamah [a], Tara M. Stewart [a], Vidhya Kumaresan [a], R. Jonathan Robitsek [a], Weiming Xia [a,c], David H. Farb [a,b,*]

[a] Department of Pharmacology & Experimental Therapeutics, Boston University School of Medicine, Boston, Massachusetts, USA
[b] Center for Systems Neuroscience, Boston University, Boston, Massachusetts, USA
[c] Geriatric Research Education and Clinical Center, Bedford Veterans Administration Healthcare System, Bedford, Massachusetts, USA
[d] Department of Biology, Boston University, Boston, Massachusetts, USA

ARTICLE INFO

Keywords:
Hippocampus
Memory
Consolidation
Place cells
Ripples
Extra-synaptic
Inhibition
α5GABAA-R
Alzheimer's
TgF344-AD

ABSTRACT

Decades of research attempting to slow the onset of Alzheimer's disease (AD) indicates that a better understanding of memory will be key to the discovery of effective therapeutic approaches. Here, we ask whether prodromal neural network dysfunction might occur in the hippocampal trisynaptic circuit by using α5IA (an established memory enhancer and selective negative allosteric modulator of extrasynaptic tonically active α5GABA-A receptors) as a probe drug in TgF344-AD transgenic rats, a model for β-amyloid induced early onset AD. The results demonstrate that orally bioavailable α5IA increases CA1 pyramidal cell mean firing rates during foraging and peak ripple amplitude during wakeful immobility in *wild type* F344 rats in a familiar environment. We further demonstrate that CA1 ripples in TgF344-AD rats are nonresponsive to α5IA by 9 months of age, prior to the onset of AD-like pathology and memory dysfunction. TgF344-AD rats express human β-amyloid precursor protein (with the Swedish mutation) and human presenilin-1 (with a Δ exon 9 mutation) and we found high serum Aβ42 and Aβ40 levels by 3 months of age. When taken together, this demonstrates, to the best of our knowledge, the first evidence for prodromal α5GABA-A receptor dysfunction in the ripple-generating hippocampal trisynaptic circuit of AD-like transgenic rats. As α5GABA-A receptors are found at extrasynaptic and synaptic contacts, we posit that negative modulation of α5GABA-A receptor mediated tonic as well as phasic inhibition augments CA1 ripples and memory consolidation but that this modulatory mechanism is lost at an early stage of AD onset.

1. Introduction

Forming new memories and reinforcing existing memories involves a synthesis of new sensory information with previously encoded information [1]. Yet how neural circuitry accomplishes this function of balancing incoming sensory information represented by excitatory and inhibitory synaptic activity into memory remains a mystery. This process can be seen most clearly in the hippocampal trisynaptic circuit (HTC). In this circuit, orderly arrayed excitatory pyramidal cells (some of which function as place cells) balance excitation with inhibition in the CA3 and CA1 regions via their nearby inhibitory interneurons. The result of these concerted actions is the synchronous output of rhythmic neural activity or sharp-wave ripples (SPW-Rs) which is thought to support spatial memory in awake and resting animals [2,3].

Hyperactivity of the HTC is associated with memory deficits such as amnestic mild cognitive impairment (aMCI) and Alzheimer's disease (AD) in humans and animals [4, 5, 6, 7, 8, 9, 10, 11, 12], raising the hypothesis that increased circuit activity underlies memory dysfunction [6, 7, 8]. Such a pathological increase in pyramidal cell excitability, commonly referred to as "hyperactivity", is thought to impair memory in older humans and animals since pharmacologically reducing the hyperactivity improves cognition in amnestic mild cognitively impaired older adults [11] and aged rats [6,12]. However, paradoxically, a well-known class of memory enhancers in adult animals [13, 14, 15, 16] (exemplified

* Corresponding author.
E-mail address: dfarb@bu.edu (D.H. Farb).

https://doi.org/10.1016/j.heliyon.2021.e07895
Received 24 August 2021; Received in revised form 27 August 2021; Accepted 27 August 2021

by α5IA) are thought to reduce inhibitory neurotransmission (in effect mimicking functional disinhibition) by preferentially reducing the activity of **α**5-containing GABA-A receptors located primarily on hippocampal pyramidal neurons [14].

To approach this apparent conundrum, we asked whether reducing tonic inhibition with α5IA, which has been shown to improve memory [13, 14, 15, 16] function, would increase CA1 place cell activity and enhance pattern separation *in vivo*. To achieve this goal, we performed *in vivo* electrophysiology experiments with a within subject design to measure real-time changes in neural network activity in the CA1 subregion as a measure of HTC output. To probe for the potential involvement of tonic inhibition as an AD-related early onset dysfunction in the hippocampal trisynaptic network we compared the dynamical responses of young adult CA1 pyramidal cells to α5IA in TgF344-AD with *wild type* F344 rats.

To the best of our knowledge, these results demonstrate, for the first time, a key modulatory role for α5GABA-A receptors in CA1 pyramidal cell mean and peak firing rates *in vivo* and ripple amplitude in young adult *wild type* rats. As ripples are known to correlate with improved remembering [17] we asked whether adult TgF344-AD rats, with high plasma levels of Aβ42 and Aβ40, would also generate CA1 ripples that are sensitive to potentiation by α5IA and thus contingent upon the activity of α5GABA-A receptors. To our surprise, however, α5IA responsivity of CA1 ripples was ablated in young adult TgF344-AD rats. These findings strongly suggest pharmacologically that extrasynaptic tonic inhibitory α5GABA-A receptors contribute to the modulation of ripple amplitude and that TgF344-AD rats exhibit prodromal disruption of this key inhibitory modulatory mechanism essential to memory function.

2. Methods

2.1. Subjects

The in vivo electrophysiological experiments reported herein were performed on n = 20 adult male rats. Escalating dose experiments looking at pyramidal cell firing rates during exploration of a familiar environment were performed in four wildtype male LE retired breeders ages 8–12 mo. Studies of CA1 place cell remapping activity in response to environmental novelty were performed in three wildtype LE male retired breeders ages 8–12 mo and three F344 males ages 8–12 mo. Investigations of dose-dependent effects of α5IA on ripple activity when animals were immobile in a familiar environment were performed in 1 LE male rat age 15 mo; 4 F344 rats ages 9–18 mo; and, 3 adult male TgF344-AD rats ages 9–16 mo. Two 11 mo old male F344 rats and one 11 mo male TgF344-AD rat were used for the vehicle control experiments.

The novel location recognition behavioral experiments were performed in separate groups ($n = 9$) of wildtype male LE retired breeders age 8–12 mo and F344 (n = 30) and TgF344-AD (n = 27) rats that had not undergone surgical implantation of microelectrode arrays.

All rats were individually housed in a climate-controlled vivarium maintained on a regular 12hr/12hr light/dark cycle in the Laboratory Animal Science Center at the Boston University School of Medicine. Rats had *ad libitum* access to water but were mildly food deprived to 85% of their free-feeding weight during training and testing. Rodent housing and research were both conducted in strict accordance with the NIH Guide for the Care and Use of Laboratory Animals. Boston University is accredited by the Association for Assessment and Accreditation of Laboratory Animal Care. The Boston University Institutional Animal Care and Use Committee approved all procedures described in this study.

2.2. Drugs

The GABA-A α5-selective positive allosteric modulator α5IA (3-(5-methylisoxazol-3-yl)-6-[(1-methyl-1,2,3-triazol-4-yl) methyloxy]-1,2,4-triazolo[3,4-a] phthalazine) (Sigma Aldrich Inc, USA and Tecoland, Irvine, California, USA) was chosen for these studies due to its unique pharmacodynamic profile. Oral administration of α5IA to rats at doses of 0.3, 1.0 and 3.0 mg/kg have all been shown to enhance hippocampus-dependent memory in the absence of locomotor, anxiogenic, or epileptogenic side effects [12]. Memory enhancing effects of α5IA occur when the drug is administered 30 min before trial commencement at which time receptor occupancy for the 0.3, 1.0 and 3.0 mg/kg doses were determined to be 25%, 55%, and 68% respectively [11]. The variance about the occupancy values in the 0.3 mg/kg dose was over three times that of the 1.0 mg/kg and 3.0 mg/kg doses [11]. The intermediate dose of 1.0 mg/kg was chosen for these *in vivo* electrophysiology studies because the occupancy percentage and variance at this dose are more favorable than those associated with a lower dose and, because the higher dose did not significantly improve performance above that shown with the 1.0 mg/kg dose on the Morris water maze [11, 12, 13] This dose was also predicted have fewer off-target effects than the higher dose.

The vehicle (0.5% 400 centipoise methylcellulose) and drug were both administered via oral gavage 30 min before initiation of testing. To facilitate the oral administration process, the rats were mildly sedated by placing them in an induction chamber filled with 5% isoflurane. The drug was always administered after vehicle; counterbalancing the order of vehicle and drug administration was not possible in this model due to the duration of the experimental protocol, the plasma half-life (0.9 h) of the drug and, our desire to record the effects of α5IA, and vehicle from the same cells in the animals on the same day to minimize electrode drift.

2.3. Microelectrode arrays

Custom microelectrode arrays constructed with a cast polymer core (Smoot-Cast 300; Smooth-On Inc., Easton, PA) and fitted with 24 independent micromanipulators permitted positioning of individual nichrome tetrodes (Sandvik, Palm Coast, Florida, USA) within the brain region of interest. Each micromanipulator consisted of a 0.5 in, 23-gauge stainless steel tube affixed with cyanoacrylate adhesive to a Delrin bridge. A flexible fused silica capillary tube (Polymicro Technologies™), was inserted into this 23-gauge guide tube and secured into position with cyanoacrylate adhesive to provide structural support for the tetrodes. A 0–90 × 0.5 in brass machine screw (J.I. Morris, Southbridge, Massachusetts, USA) was attached to a Delrin bridge and used to facilitate vertical movements of the microdrive. Twenty-four stainless steel 30-gauge guide tubes were inserted in the polymer core to provide additional support for the silica capillary tubes. These tubes where bundled together at the bottom of the microarray by insertion into a 1.0 cm piece of 14-gauge stainless tubing. The entire bundle of guide tubes was then sealed with dental acrylic to create a de facto mounting point for subsequent surgical implantation of the completed microarray. Each tetrode was comprised of four nichrome wires (California Fine Wire, Grover Beach, CA, USA); the tips of which were gold plated to decrease impedance to 200 kΩ at 1 kHz.

The F344 and TgF344-AD rats used in the vehicle control experiments were all implanted with Buzsaki 32 type silicon probe microelectrode arrays (NeuroNexus, Inc. Ann Arbor, Michigan, USA) affixed to a custom micromanipulator.

2.4. Surgical procedures

Rats were anesthetized with isoflurane (3.5% for induction; 1.5%–2% thereafter) in 100% oxygen delivered via a calibrated vaporizer (Vaporizer Sales & Services Inc., Rockmart, Georgia, USA). Buprenorphine (0.05 mg/kg, s.c.) was administered 30 min before surgery to provide intraoperative analgesia. Glycopyrrolate (0.02 mg/kg, subcutaneous; s.c.) was also administered to reduce salivary and bronchial secretions and prevent vagal bradycardia. The heads of the animals were shaved and prepped for surgery with betadine in triplicate. After placing the rats in a stereotaxic instrument (David Kopf Instruments, Tujunga, CA), a midline sagittal incision was made across the top of the head to expose the cranium. A small craniotomy (~2 mm in diameter) was

created immediately above the right dorsal hippocampus at 3.6 mm AP and 2.6 mm ML from bregma. The dura mater was excised and the electrode array lowered into position above the surface of the neocortex. Ten additional holes (<0.5 mm) were drilled into the skull for the placement of an equal number of stainless-steel screws; two of these screws served as electrical grounds as well as providing additional anchoring points for securing the microelectrode array to the skull with dental acrylic (Patterson Dental Supply, St. Paul, Minnesota, USA). At the end of surgery, electrodes were advanced ~750 μm into the cortex. The craniotomy was sealed using Kwik-Sil silicone sealer (World Precision Instruments, Shanghai, China) for tetrodes or a warm melted mixture of parafin wax and mineral oil for silicon probes. Post-operative analgesia was maintained for 72 h with buprenorphine (0.05 mg/kg, s.c.). Lactated ringers (6ml every 12 h), soft food, and Hydrogel (ClearH2O, Westbrook, Maine, USA) were also administered during the first 72 h after surgery to ensure adequate caloric intake and hydration. Topical triple antibiotic and Cephalexin (60 mg/kg, p.o.) were administered for seven days post-operatively to reduce the risk for infection at the implant site.

2.5. Data acquisition and spike sorting

Recordings of place cell and local field potentials (LFPs) were acquired from custom nichrome tetrode microarrays or Buzsaki 32 channel type silicon probes (NeuroNexus, Inc. Ann Arbor, Michigan, USA) using a 96 channel Plexon Multichannel Acquisition Processors (Plexon Inc., Dallas, TX) and an Intan RHD system respectively. Recordings were referenced to a common skull screw for LFPs, or an indifferent tetrode (for single unit activity), and hardware filtered for LFPs (0.77–400 Hz) and spikes (154 Hz–8.8 kHz). LFP signals were amplified 1000X and digitized at 1 kHz while spike signals were amplified 2000–8000X and digitized at 40 kHz. The location of the rat within each environment for recordings of place cell activity was tracked in real-time with an overhead camera imaging two LEDs connected to the headstage (HST/32V-G20-2LED) at a rate of 30 frames/sec (Cineplex, Plexon Inc., Dallas, Texas, USA). The appearance of theta activity during ambulation and ripple events in the LFPs when animals were immobile was used to functionally confirm electrode location within the CA1 hippocampal subregion. If pyramidal cell activity was not identified on an electrode during daily screening, it was advanced and allowed to settle for at least 1 h before further assessment for single unit activity.

Shareware (KlustaKwik) developed by Ken Harris [21] was used to sort action potentials into clusters based on three principal components using an expectation-maximization algorithm. Only well-defined clusters with clear refractory periods having an interspike interval greater than 1 ms were included in the final analysis. Clusters from pyramidal cells were differentiated from interneurons based on firing rates, waveform widths (≥300 μs for pyramidal cells; < 300 μs for interneurons) and the presence or absence of a burst of activity in the 3–10 ms range on inspection of the auto-correlograms [21].

2.6. Escalating cumulative dose paradigm for analysis of CA1 hippocampal pyramidal/place cell activity

Rats were allowed to explore a black plywood square (60 cm × 60 cm) enclosure with vertical yellow stripes on one wall for at least 10 days to establish this as a "familiar environment". The environment was centered on a table with a solid black impervious floor, which was surrounded by blackout curtains to mask background cues. The floor of the environment was cleaned with 30% ethanol between sessions to remove olfactory cues. Crushed fruit-flavored cereal crumbs were randomly distributed over the floor of the recording chambers to encourage continuous ambulation and exploration of the entire environment. The dosing schedule used in this model was selected based on previously reported benzodiazepine receptor occupancy over time following oral administration of α5IA [11, 12, 13]. To achieve total cumulative *in vivo* systemic doses of 0.3 1.0 and 3.0 mg/kg, the drug was administered via the oral gavage 30 min before the beginning of each recording session at concentrations of 0.0, 0.3, 0.7 mg/kg and 2.0 mg/kg. This cumulative dosing schedule combined with a within-subject repeated-measures design facilitated recording the dose-response curve for CA1 pyramidal cell (n = 60) neural activity from the same cells on a single day during four serial 10-minute recording sessions acquired while animals foraged for food in the familiar environment. Between sessions rats were placed in holding container (30 cm × 30 cm x 45 cm) which was gently rotated for ~3 min to disorient the animals immediately before placing them into the next environment. Rats had the opportunity to drink water between environmental exposures [4,6,22]. Only data from animals that showed good coverage of all four environments during was included in final analysis (see Fig S1). The average speed in meters per minute for each animal in each session of these experiments was also calculated. The Freidman's test revealed no significant difference in average speed across sessions (p = 0.3426) (see Fig S2 and Table S1).

2.7. Environment-dependent place cell remapping paradigm

During the training phase of the remapping experiments, rats were again allowed to explore a black plywood square (60 cm × 60 cm) enclosure with vertical yellow stripes on one wall for at least 10 days to establish this as a "familiar environment". During the test phase, place field remapping was assessed as the animals explored a "novel environment" (hexagon or cylinder with the same pattern of vertical stripes) in addition to the now familiar environment in the following order: Familiar–Novel–Novel–Familiar (Fig S3). All other procedures were identical to those described above for the escalating dose experiments performed in the familiar environment.

2.8. Place cell firing analysis

Place cell activity was recorded from three LE male rats while the animals explored the Familiar–Novel–Novel–Familiar environments. Pyramidal cells in the CA1 hippocampal subregion that fired at least 60 action potentials during each of the 10-minute recording sessions (minimum rate 0.1 Hz) were analyzed for place fields using a series of custom MATLAB (Mathworks, Natick, MA) scripts developed in our laboratory. Occupancy-normalized spatial firing rate maps from F344 and LE rats showing good coverage of the environments based on trajectory data (Figures S3 and S4) were estimated using the total number of action potentials (spikes) occurring in a given bin divided by the total amount of time spent in the bin (3.5 cm × 3.5 cm), with distinct firing rate maps calculated for each exposure to the familiar and novel environments. The unsmoothed and smoothed values for each bin were calculated as the mean for each bin, and all bins within 5 cm, where each bin was weighted by its distance from the central bin using a two-dimensional Gaussian kernel [23]. Bins included in the analysis must have been visited at least once during the session. Place fields were defined as six adjacent bins with averaged binned rates above 0.5 Hz and averaged binned firing rate > 2x mean overall firing rate (all bins). Data was only included for spikes that occurred when running speed was >2.0 cm/s. For each environment, the pixel-to-pixel correlations, and the spatial selectivity were calculated only if the overall mean firing rate was >0.1 Hz.

2.9. Place field analysis

To evaluate the effects of environment and treatment with α5IA on place cell characteristics we applied measures to assess for discharge frequency (mean and peak firing rates). Selectivity and stability of place cell firing, across environments under the two treatment conditions was also determined by calculating the 1) place field area, 2) spatial information content, 3) and spatial correlations, for each place cell.

1) PLACE FIELD AREA was computed for each environment as the sum of all bins that met the place field criteria. Prior to this computation,

the firing rate maps for the novel environments were transformed to a square shape to facilitate comparison with the familiar environment [24].

2) SPATIAL INFORMATION CONTENT provides a measure of the amount of information each spike conveys about the animal's position in the environment (in units of bits/spike) [25].

$$\textit{Information per spike} = \sum_{i=1}^{n} P_i\left(\frac{\lambda_i}{\lambda}\right)\log_2\left(\frac{\lambda_i}{\lambda}\right)$$

where $i = 1,\ldots, n$ is the bin number, P_i is the probability of occupancy at bin i, λ_i is the mean firing rate for bin i, and λ is the overall mean firing rate of the cell.

3) SPATIAL CORRELATIONS were evaluated by computing the bin-to-bin Pearson correlation between environments (F1 v. F2; N1 v. N2; F1 v. N1). Confidence intervals of the correlations were determined after applying the Fisher z transform which were then transformed back and reported as the as means ± SEM [26]. Previous studies have shown that place fields in the CA1 subregion are not only environmentally specific, but that once established, these place fields are very stable [27]. Based on these previous findings, only place cells with well-correlated place fields ($r > 0.5$) in the familiar environment demonstrating that these place fields were stable under both treatment conditions were used to asses for the effects of environmental novelty on place field remapping based on changes in spatial correlations.

$$z = \frac{1}{2}ln\left(\frac{1-r}{1+r}\right)$$

2.10. Cell by cell analysis for rate remapping

Individual CA1 place cells recorded from LE male rats were defined as showing rate remapping if the average in-field mean firing rate change in the two novel environments was 50% or more above or below the average in field mean rate in the two familiar environments (see Supplementary data, Table S11 & Fig. S13).

2.11. Escalating cumulative dose paradigm for analysis of ripples

A cumulative escalating dosing schedule was used to assess for within subject effects of α5IA on ripples in the CA1 hippocampal pyramidal subregion of adult male LE, WT F344 and TgF344-AD rats to minimize the

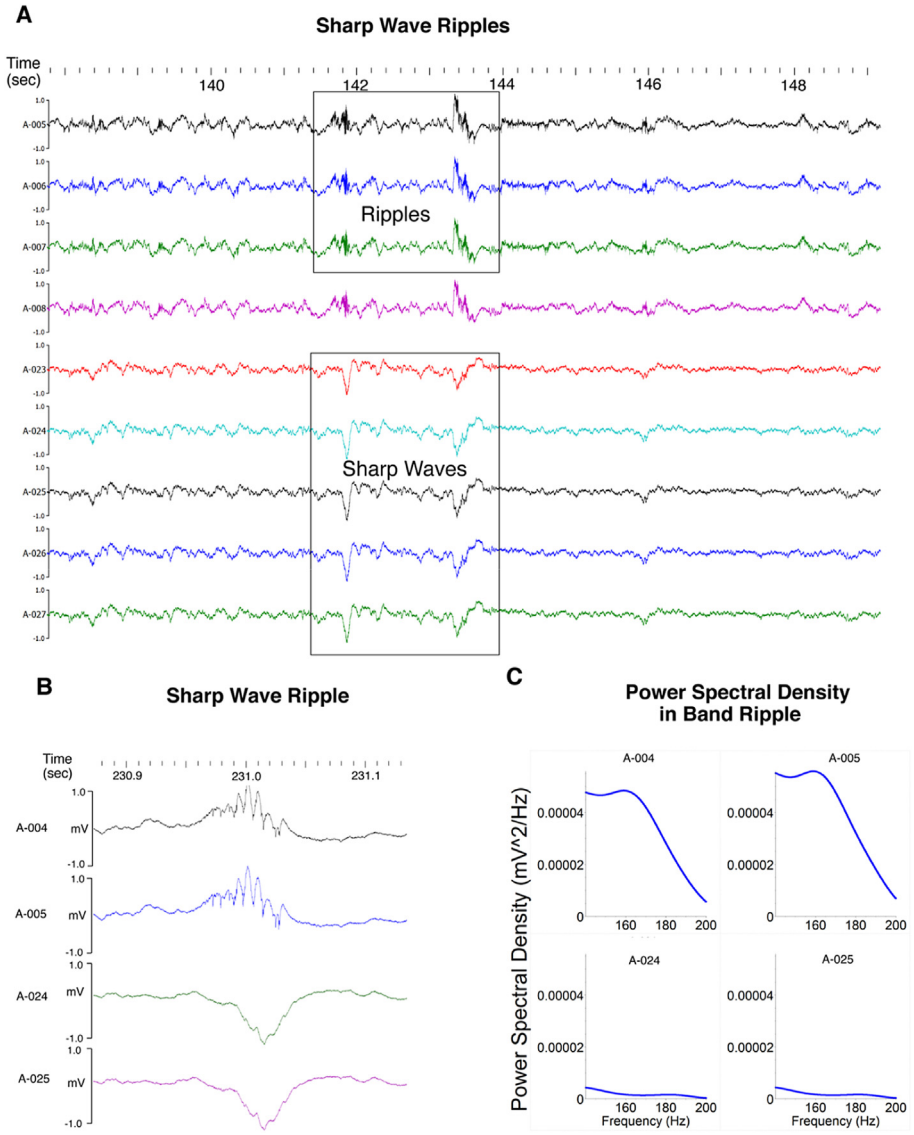

Figure 1. Sharp waves ripples. A. Distinct depth dependent characteristic oscillations (e.g., high-frequency ripples events and low-frequency sharp waves) and synchronicity of activity across recording sites is observed. B & C. LFP and power spectrum for sharp wave ripples recorded with two electrodes showing greater ripple band power (top traces and panels) and lower power on the two detecting the associated sharp wave.

influence of environmental novelty on ripple events, serial 10-minute recordings of LFPs were acquired while animals were awake and immobile in the familiar environment Food was withheld to discourage ambulation (see supplemental Fig S5 and Table S2). Localization of electrodes was based on visual examination of LFP oscillations for distinct oscillations (e.g., high-frequency ripples events and low-frequency sharp waves) and observing synchronous activity across recording sites (see Figure 1). Because our initial experiments in the LE animal did not reveal a significant increase in full session ripple band power as compared as with vehicle following the 3.0 mg/kg dose, the decision was made to reduce the maximum dose to 2.0 mg/kg in all subsequent experiments in the WT F344 and TgF344-AD rats. The cumulative dosing concentrations were adjusted to 0.0, 0.3, 0.7 and 1.0 mg/kg to achieve total cumulative *in vivo* systemic doses of 0.3, 1.0 and 2.0 mg/kg. Recordings were made for 10 min while rats were immobile resting quietly in one location of a familiar environment. Because electrode depth can influence power in ripple band, the electrodes were not moved during these recordings (see Figure 1B and C). With the exception of food being withheld to avoid stimulating ambulation, all other procedures were identical to those described above for the *escalating*-dose firing rate analysis experiments (all of which were performed in the same familiar environment). To address reproducibility and rigor of our methodology, a series of control experiments were performed to validate this protocol (see Figs. S14-16 and Tables S12 & 13).

2.12. Local field potential signal processing

Prior to statistical analysis, LFPs were frequency filtered to capture activity in the 100–250 Hz frequency band and plotted visual presentation of overt differences in ripple band (140–200 Hz) power at each dose. The effects of α5IA on peak ripple amplitude, peak ripple frequency and ripple duration were quantified using the LFP data from the electrode best positioned in the CA1 pyramidal cell layer at vehicle baseline. Electrodes were not moved between test sessions. Data was filtered for periods of wakeful immobility based on the delta (1.5–4 Hz) to theta (4–10 Hz) power ratio [27, 28] (Fig. S6 and Table S3). To identify ripples, the LFP signal voltage was bandpass filtered (140–200 Hz), squared and normalized. A custom MATLAB script validated against manually curated sharp wave ripple events was used to detect ripples. To ensure that selected events were genuine ripples, only events that deviated from the background voltage by more than 5 standard deviations (SD) at their center were defined as ripple centers [29]. Ripple boundaries defined by deviations greater than 2 SD. To further ensure that ripple detected were not false positive events, we determined the single unit firing times relative to the onset time of all ripples (Fig S7). Ripples with inter-ripple spacing less than 30 ms were merged, while those events shorter than 20 ms or longer than 100 ms excluded. The dose dependent change in raw power for each FFT frequency was defined as the dependent variable of interest (n) and compared with itself across all 4 doses tested. All PSD data are reported in mV^2/Hz and analyzed using a within subjected repeated measures ANOVA.

2.13. Histology

At the end of the study, rats were deeply anesthetized with pentobarbital (100 mg/kg; i.p.) and the recording electrode locations marked by passing anodal current (30 μA, 5 s) through each wire of the tetrodes. The animals were then perfused with ice cold phosphate buffered saline (7.4 pH) followed by fresh 4% paraformaldehyde. Brains were extracted and post-fixed at 4 degrees C, cryoprotected in 15 and 30% sucrose. All brains were inspected for and found to be devoid of lesions and tumors. 30 μM sections were obtained and Nissl stained prior to microscopic inspection and imaging (Fig. S8).

2.14. Quantification of plasma Aβ

Blood samples (200–250 μl) were taken from the tail veins of F344 (and TgF344-AD rats. Plasma samples (100 μl) were prepared using 10% potassium K-EDTA mixed with whole blood at final 0.1% K-EDTA dilution. Blood sample were centrifuged at 1500g to extract supernatant plasma. Prepared plasma samples were stored at -80 °C for subsequent biochemical analysis with ELISA. A Meso Scale Discovery (MSD) platform was used to test the samples. Assays for Aβ 40 and 42 were analyzed using V-PLEX Aβ peptide Panel 1, following the manufacturer's instructions (MSD, Gaithersburg, Maryland, USA). An analysis of the variance with Kruskal-Wallis test for plasma concentrations of Aβ42 and Aβ40 in WT F344 and TgF344-AD revealed no significant differences due to sex. Data from males and females was therefore merged prior to analysis for effects of genotype on Aβ42 and Aβ40 (Table S4).

2.15. Location novelty recognition task

The Location Novelty Recognition Test (LNRT) was performed using a separate group of unimplanted animals as internal control experiment only for the purpose of confirming observations from previous reports indicating α5IA enhances memory function. These data were not relied upon to arrive at any conclusion based on *in vivo* electrophysiological studies of the neural correlates of memory function. The LNR test is a simple test of memory function that relies on the rat's innate exploratory behaviors to assess the ability of the animal to recognize that an object is in new location without having to employ any rules or behavioral reinforces. In the current study, animals were acclimated to the same familiar environment used in the *in vivo* electrophysiological studies. During the training trial two copies of the same object were placed in two different quadrants of the familiar environment and the animal was allowed to explore these objects for 10 min. Following a two-hour delay, one of the two objects from the training trial was moved in a novel location in a previously vacant quadrant and the animal was reintroduced to this environment and once again allowed to explore the objects for 10 min. The preference for novelty is revealed by the tendency of the animal to spend more time exploring the displaced object. Two identical objects were used in a given vehicle drug training and test session but, different objects were used for each rat to ensure counter balancing for differences in the complexity of the object. All objects were tested prior to the beginning of these experiments and found to be devoid of bias – rats spent equal time with each of the objects used. The environment floor and objects were cleaned with 30% ethanol between recordings to remove olfactory cues. A location discrimination index was calculated for each trial as previously described [30, 31]:

$$Location\ Index = \frac{(T_{NOV} x 100)}{(T_{NOV} + T_{FAM})}$$

where, T_{NOV} is the time spent exploring the displaced object and T_{FAM} is the time spent exploring the non-displaced object. A one-sample *t*-test was used to determine whether the location index was different from chance level performance (50%) and the performance of each rat in either treatment group was directly compared using a paired, one-tailed *t*-test with a probability level of $\alpha < 0.05$ considered to be statistically significant.

Validation of Objects used for the LNRT: Each type of object was evaluated for intrinsic bias by comparing the time spent exploring the type of object with the other objects using the one-way Wilcoxon Test (Table S5 and Fig S9). Object 1 (deodorant bottle); Object 2 (bubbles bottle); Object 3 (salt shaker); Object 4 (doll). All objects were thoroughly cleaned, and filled with lead pellets to anchor them in place during trials. The results of a Kruskal-Wallis test comparing the time spent exploring each of the four different types of objects with each other was not significant ($p = 0.21$) ensuring that rats spent a similar amount of time interacting with each. None of the objects included in these studies had a negative or positive intrinsic value. Animals showed no aversion to any of the objects used in these studies.

2.16. Statistical analysis of data

The unit of analysis for each comparison was selected based on the dependent variable interest. The unit of analysis of the escalating dose, place cell remapping activity and cell by cell comparisons was the single pyramidal cell or interneuron. The unit of analysis for LFPs power at each frequency was an FFT point. The unit of analysis for the location novelty recognition behavioral testing was an animal. Data were analyzed for normality prior to statistical analysis using the Kolmogorov-Smirnov test. Normally distributed data was analyzed for within subject effects using a parametric paired subject t tests and repeated measures ANOVAs with Bonferroni corrections for multiple comparisons. The non-parametric Wilcoxon Signed Rank test, Kruskal-Wallis test and Friedman's ANOVA were used for analysis of data that was not normally distributed. Planned comparisons were performed based on dose-dependent *a priori* expected effects of drug-mediated disinhibition on mean and peak firing rates, spatial information content (SIC), and LFP power all of which have previously been shown to be sensitive to drug-induced changes in inhibition and excitation. All results are expressed as the mean ± SEMs with an alpha $p < 0.05$ significance level unless otherwise indicated. The alpha level was adjusted accordingly for the number of multiple comparisons being made in a repeated measures analysis. All statistical analyses were performed using the SPSS Statistics Program for Macintosh, Version 20.0 (IBM Corporation, Armonk, NY, USA). Figures were generated using GraphPad Prism (GraphPad Software, La Jolla California USA).

3. Results

3.1. Reducing α5GABA-A receptor activity increases CA1 pyramidal cell firing rates in young adult rats

α5IA is known to cause disinhibition via a GABAergic mechanism from cell culture and hippocampal slice experiments *in vitro* [12]; however, it is unknown what effect this inhibitor of α5GABA-A receptors would have on intact circuitry *in vivo* using freely moving animals [2]. We hypothesized that if α5IA acted via disinhibition then it would potentiate pyramidal cell firing rates in the CA1 layer of wild type adult male Long Evans (LE) rats. To test this hypothesis, we recorded the activity of CA1 pyramidal cells using chronically implanted microelectrode arrays while rats foraged for food in a familiar environment. We used a within subject design so that each animal served as its own control. Each animal was administered vehicle followed by 3 ascending doses of α5IA (Figure 2A, S10, Table S6). Administration of α5IA significantly increased mean CA1 pyramidal cell mean firing rates (MFR) at the 0.3 mg/kg dose ($p = 0.002$, two-sided signed rank test), 1 mg/kg dose ($p = 0.001$) and 3 mg/kg dose ($p < 0.0001$) (Figure 2B). Potentiation appeared to level off above 1.0 mg/kg, consistent with a receptor occupancy model established previously (Figure 2C) Such an increase in MFR is typically referred to as hyperactivity [6,7] and thought to impair memory function as described above, yet α5IA is known to act as an enhancer of spatial memory in the Morris water maze [12].

3.2. α5IA-induced excitability of CA1 place cells does not increase or decrease place field remapping in adult rats

Theories about the cellular basis for memory are rapidly evolving, with one view that subtypes of pyramidal cells such as "place cells" are differentiated from the bulk of pyramidal cells. Having established that α5IA enhances CA1 pyramidal cell mean firing rates using electrophysiology and enhances spatial memory using a behavioral test, we asked whether place cells would become hyperactive or whether they would respond differently as a function of local network activity. Lastly, we asked whether place cells would exhibit environment-dependent spatial remapping, a characteristic of the HTC believed to be a proxy for memory formation [6]. Multiple single units were recorded from the CA1 pyramidal cell layer of 3 adult F344 rats (Place cell n = 152) while the animals foraged for food in familiar and novel environments (Figure 3A). As

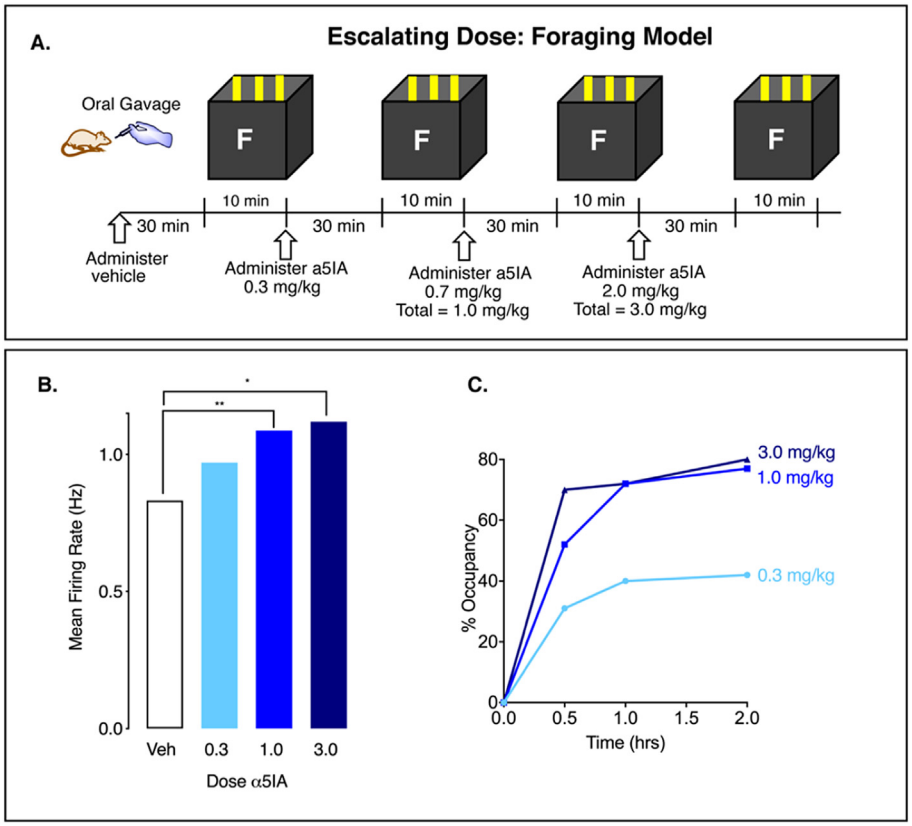

Figure 2. α5IA enhances LE CA1 pyramidal cell firing rates in a familiar environment. A. Within subjects escalating dose experiment in a foraging model. B. α5IA increases MFR immediately following oral administration, consistent with the dose response relationship of α5IA in panel C. **C.** Percent occupancy determined by *in vivo* dosing and *ex vivo* ligand binding levels off at 1.0 mg/kg drug (data replotted from refs 11, 12). One-way repeated measures ANOVA shows dose-dependent increase in MFR (*p = 0.02; **p = 0.003; see supplemental Table S6). Data from 4 adult male LE rats.

anticipated, α5IA (1.0 mg/kg, p.o.) increased the average mean firing rate of place cells in the familiar environment (Figure 3B; planned comparisons). In the novel environment, MFR and In-field MFR increase as expected in response to novelty (Figure 3B). The average peak firing rate (PFR) (Figure 3C), and mean in-field firing rate (Figure 3D) also increase in the familiar environment. However, no significant interaction between drug and environment was observed.

Spatial information content (SIC) decreases in the novel environment, which is not affected by drug (Figure 3E). Place field area (PFA) significantly increases with environmental novelty in both treatment conditions, indicating an effect of environment (Figure 3F). Moreover, place field spatial correlations between the familiar and novel environments in both the vehicle and drug demonstrate that remapping occurred in both treatment conditions (Figure 3G). Comparisons of spatial correlations between the two familiar environments across treatment conditions is not significant ($r_{veh} = 0.77 \pm 0.12$; $r_{drug} = 0.76 \pm 0.13$; $p = 0.86$), demonstrating that α5IA administration has no significant effect on the stability of well-established highly correlated place fields. The tests for interaction between drug and environment were not significant.

Despite enhancing CA1 place cell firing rates, α5IA had no effect on the spatial remapping of place cells, as quantified by the place cell spatial correlation measurement (Figure 3G). The SIC per action potential of place cells also was not significantly affected by α5IA (Figure 3E), nor was the place field size (Figure 3F). Surprisingly, we found no enhancement of place cell remapping by α5IA, even though we observed significant improvement on the novel location recognition test, both tests thought to evaluate spatial memory. Similar findings were observed in a group of wild type LE adult male rats **(see** supplemental data section Figs. S11, S12 & Tables S7 - S9).

3.3. Location novelty recognition test performance of wild type and TgF344-AD rats

The effect of treatment with oral α5IA (1.0 mg/kg) on Locational Novelty Recognition (LNR) test performance was assessed using a within subject design in a separate group of unimplanted LE male rats (n = 9) (Figure 4A and B). Vehicle LNR test was followed by a 3-hour delay in the home cage, after which the test for α5IA effects on performance was assessed. Treatment with α5IA significantly improved performance of LE rats on this task, a finding which is consistent with previous reports of this compound enhancing memory function [12,13] (Figure 4C).

Next the memory functions of unimplanted adult F344 (n = 30) and TgF344-AD (n = 27) rats age 9–18 mo, were compared in between subject design experiment. For this test, the training interval duration on the LNRT was reduced from 10 to 3 min and the delay between training and testing sessions was reduced from 2 h to 20 min. The same previously validated objects and familiar enclosure used in the experiments assessing for α5IA effects on memory performance in LE were used in this test but without drug. The shorter training interval and delay between training and testing were selected based on previous reports indicating that F344 rats spend more time exploring the object in the novel location in this model [17]. TgF344-AD rats avoided the novel object more often than F344 rats (TgF344-AD (7/27 or 26%) vs F344 (2/30 or 7%)). Analysis of the data with these novelty avoiding rats included suggested

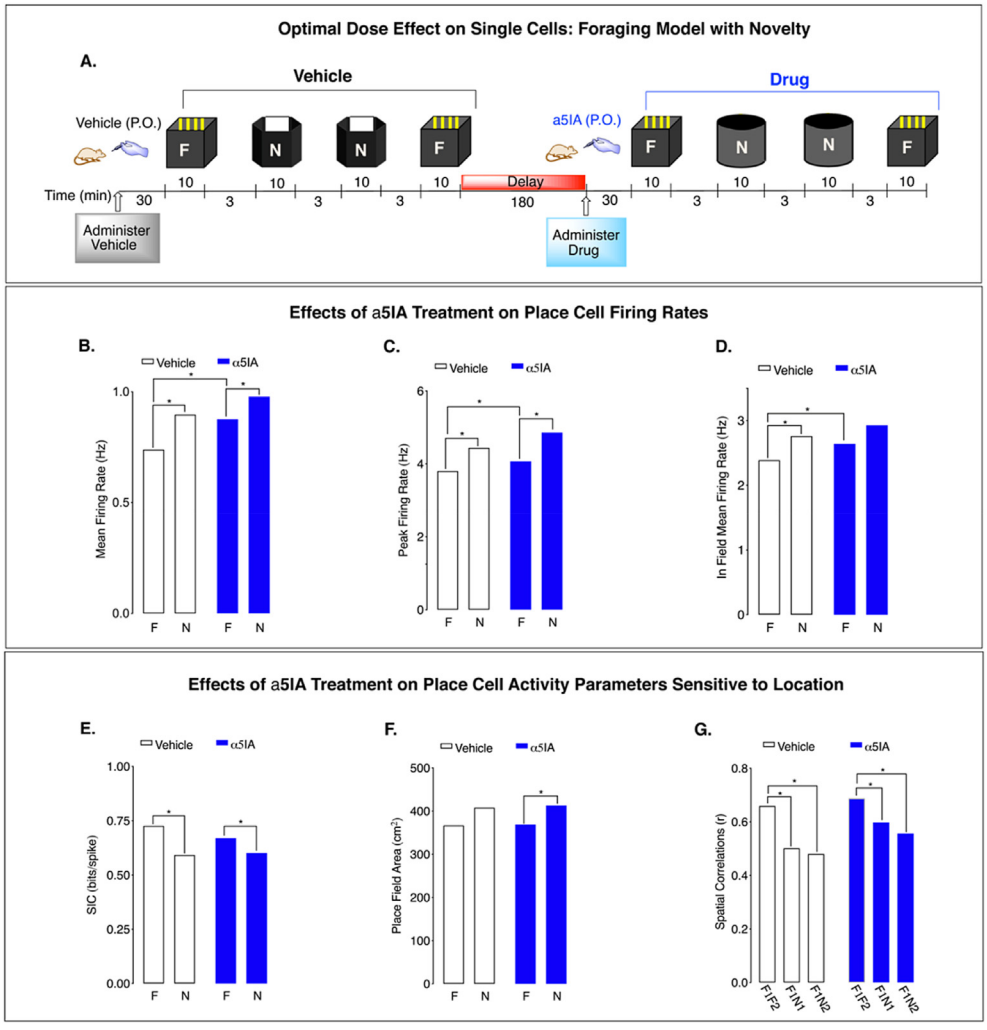

Figure 3. α5IA increases CA1 place cell activity in adult F344s. A. Environment-dependent remapping of place fields recorded across successive sessions. Administration of α5IA (1.0 mg/kg, p.o.): B. increases MFR of CA1 place cells in a familiar environment; C. increases PFR in a familiar environment, D. increases In-field MFR in a familiar environment, E. has no effect on SIC in familiar or novel environments, F. has no effect on PFA in familiar or novel environments, and G. no significant effects treatment on place field spatial correlations upon exposure to environmental novelty. Significance: *p < 0.05. Data from 3 young adult F344 male rats.

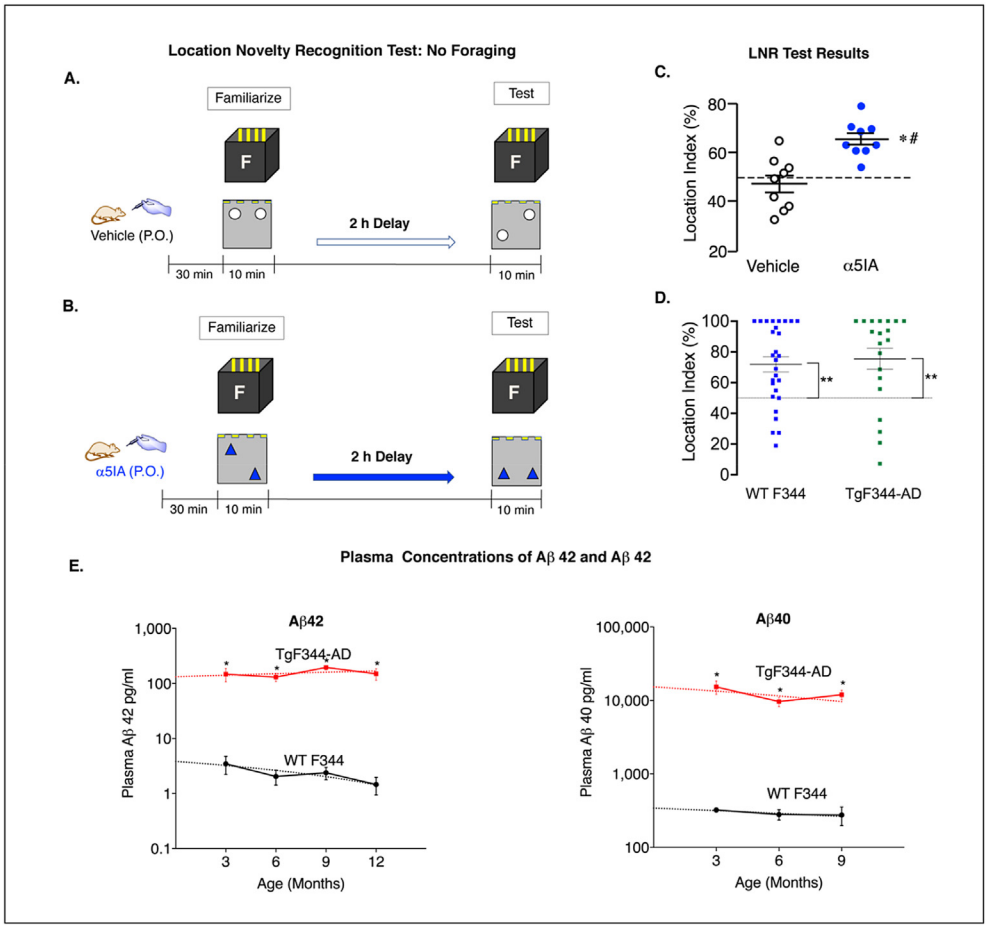

Figure 4. TgF344-AD rats expressing high plasma Aβ42 levels fail to distinguish location novelty. A & B. Models used for assessing LNRT performance following vehicle and α5IA (1 mg/kg) administration. C. Location index scores for individual LE rats ($n = 9$) following administration of vehicle and α5IA. α5IA improved performance above chance level (dashed line; #$p < 0.001$) and above actual performance of at vehicle baseline (*$p < 0.001$). D. Location index scores of F344 and TgF344-AD rats showing both groups of rats spend more time exploring the object in the novel location. Significance: ** at $p < 0.001$. E. Mean plasma Aβ42 increases 4100% - 10,000% are seen at ages 3, 6, 9, and 12 mo TgF344-AD rats as compared with F344. Mean plasma Aβ40 is also increased also similarly increased at 3, 6, and 9 mo in TgF344-AD rats (green) vs F344 controls (black). Significance: * at $p < 0.01$.

that F344 rats spent significantly more time exploring the object in the novel location (F344, $p = 0.0053$; TgF344-AD, $p = 0.4737$). However, when the rats that avoided the object in the novel location were removed from the analysis, both groups of rat spent more time exploring the object in the novel location (F344 ($n = 30$), $p = 0.0003$; TgF344-AD ($n = 20$), $p = 0.0019$). In addition, the results of Mann-Whitney test revealed no significant difference in performance between the two groups of rats on this test ($p = 0.5068$) indicating no memory deficits in TgF344-AD rats aged 9–18 months. These results are consistent with those of previous studies of recognition memory function in TgF344-AD animals which also did not find significant memory deficits prior to 18 months of age [17] (Figure 4D). Increased plasma concentrations of Aβ42 and Aβ40 are associated with the performance deficits on the LNRT observed in TgF344-AD rats (Figure 4E).

3.4. α5IA enhances the ripple-band power spectrum in F344 but not TgF344-AD rats

At this point we decided to focus on an aspect of HTC output as a surrogate *in vivo* biological marker of memory function. Specifically, the ripple-band frequencies (140–200 Hz) generated in CA1 and transmitted to the prefrontal cortex contain encoded information about past circuitry activity. We chose to focus on activity in the ripple band because ripples have been shown to participate in memory consolidation and are known to be coordinated by a consortium of GABAergic interneurons [2].

Based on observations from place cell activity analyses showing no significant increases in SIC or other metrics of spatial remapping such as place field size or spatial correlations, the effects of α5IA on ripples were investigated using *in vivo* electrophysiological recordings of LFPs acquired while animals were awake and immobile in a familiar environment. This behavioral model reduces theta modulation and minimizes the effects of environmental novelty and memory task demands, while at the same time promoting ripples. Specifically, we recorded LFPs from F344 and TgF344-AD male adult rats following administration of vehicle or α5IA in a paradigm that minimizes both novelty and mobilization. In F344 rats, α5IA increases ripple band power in a dose-dependent manner with the largest increase of 43% occurring at 1 mg/kg (Figure 5A). By contrast, TgF344-ADs showed a decrease in ripple band power following oral administration of 1.0 mg/kg α5IA (Figure 5B). Comparison of F344 and TgF344-AD for dose-response effects of α5IA revealed that the increase in ripple band power seen in F344 rats did not occur in TgF344-ADs which continue to show a pattern on serial exposure to the familiar environment after drug administration that was strikingly similar to that seen under vehicle control conditions (Figure 5 C-E).

The frequency distributions for ripple event peak amplitudes reveals skewed distributions in both F344 and TgF344-AD subjects (Figure 5F). α5IA shifts the frequency distribution to the right in F344 but not TgF344-AD animals. This is consistent with the observation that α5IA increases the mean peak amplitude of ripples in F344 but not TgF344-AD rats (Figure 5G). Interestingly, TgF344-AD genotype increases the average peak ripple amplitude at baseline to a level that matches the effect of α5IA on F344s. The effects of α5IA on other ripple parameters were also evaluated though a discussion of the results would be beyond the scope of this report (See supplemental Figs S17 - S19 and Tables S14 -S16). It is tempting to propose that this increase in CA1 ripple amplitude may be a compensatory prodromal response to early, potentially memory impairing, effects of circulating beta-amyloid.

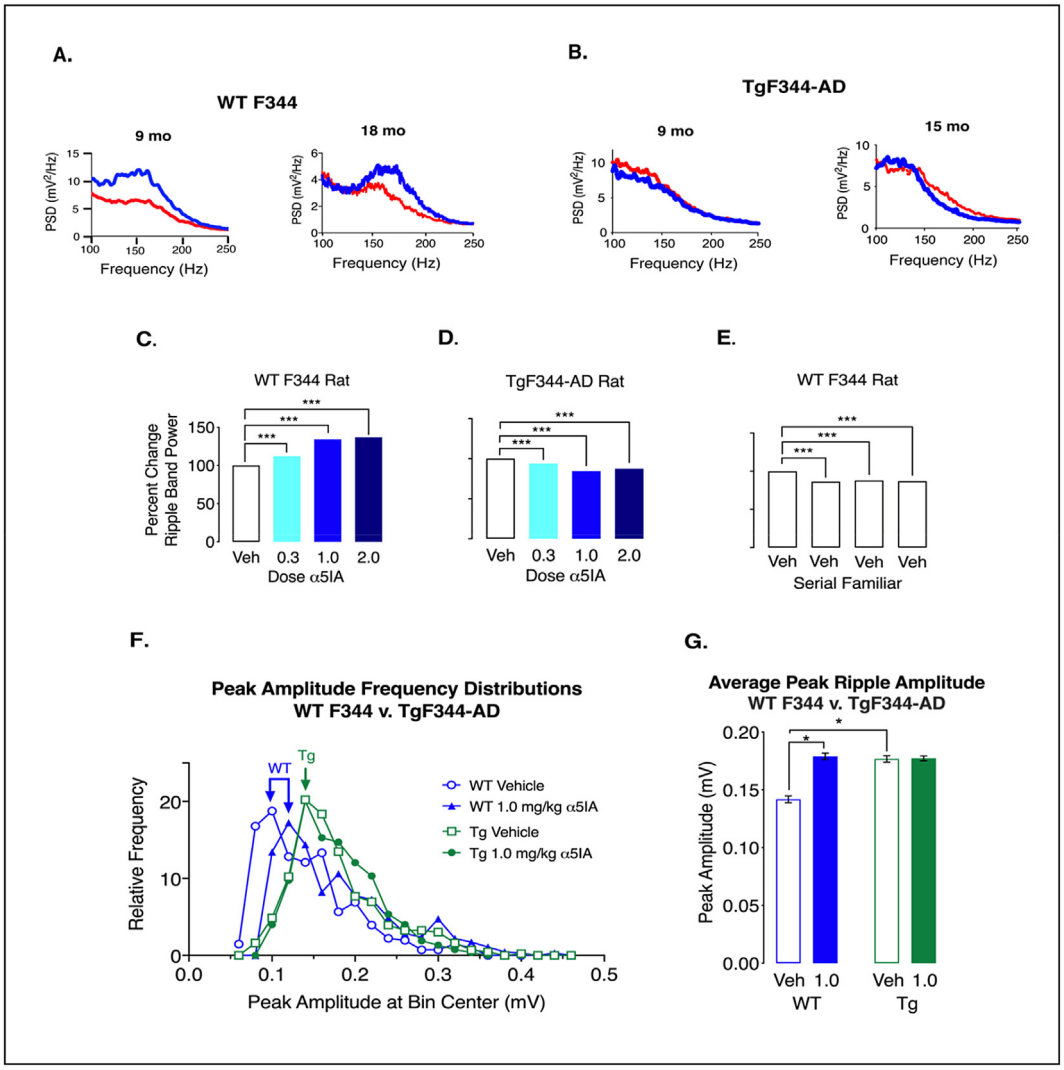

Figure 5. Administration of α5IA does not increase ripple band power or peak ripple amplitude in TgF344-AD Rats. A. Visual comparison of the spectrums (top panel) from representative well-positioned electrodes in two F344s age 9 & 18 mo reveals a remarkable overt increase in ripple band power following administration of α5IA (1.0 mg/kg). B. Visual inspection of the power spectrums from well-positioned tetrodes adult TgF344-AD rats age 9–15 months demonstrates a decrease in ripple band power following administration of α5IA. C. Histogram showing percent increase in ripple band power in F344 rats following administration of escalating doses of α5IA. D. Histogram showing percent decrease in ripple band power in TgF344-AD rats following administration of escalating doses of α5IA. E. Percent decrease in ripple band power in adult F344 rats following administration of vehicle only during serial exposures to a familiar environment. F. Peak ripple amplitude frequency distributions in F344 before and after oral administration of 1.0 mg/kg α5IA (n = 3) show a shift to the right that is not seen in TgF344-AD rats (n = 3). G. Peak ripple amplitude significantly increases in F344 following 1.0 mg/kg α5IA. In addition, peak ripple amplitude is significantly greater under vehicle conditions in TgF344-AD rats as compared with F344s. Significance: * at $p < 0.05$, **$p < 0.01$, and ***$p < 0.001$.

4. Discussion

The current observations in TgF344-AD (as compared with F344) rats reveal a significant prodromal increase in CA1 peak ripple amplitude that is nonresponsive to α5IA, consistent with a homeostatic prodromal response to early stage effects of circulating beta-amyloid. The present findings are associated with significantly elevated plasma concentrations of Aβ42 and Aβ40 in TgF344-AD rats, implicating bioaccumulation of Aβ as the likely active principle in neural circuitry dysfunction reported here.

This hypothesis of prodromal disruption of HTC network function in AD is consistent with the finding that ripple amplitude predicts which information is remembered [18] and that disruption of SPW-Rs during rest impairs spatial learning [19]. When non-human primates perform memory-guided visual search tasks the SPW-Rs associated with trials that are "remembered" have larger amplitudes than do the SPW-Rs associated with trials that are "forgotten" [18]. By contrast, the duration of SPW-Rs does not change based on whether a trial is remembered or forgotten. These results establish a relationship between SPW-R amplitude and which trials are remembered. Chronic circuitry level hyperactivity due to the loss of functional GABAergic interneurons has been proposed to underlie memory dysfunction associated with age-related mild cognitive impairment [20]. Yet acute administration of levetiracetam plus valproic acid rapidly reverses the memory impairment in aged rats [12] and chronic hyperactivity as measured by decreased mean firing rate, increased spatial information content, and place field sharpening to be indistinguishable from young adults [6]. These observations suggest that the HTC may very well be morphologically intact but physiologically dysfunctional resulting in resistance to a nootropic drug.

In conclusion, these findings indicate that plasma Aβ burden increases peak ripple amplitude and decreases the ability of tonic extrasynaptic and/or synaptic α5GABA-A receptor mediated inhibitory modulation of ripple dynamics in the CA1 subregion. To the best of our knowledge this may represent the first investigation of α5GABA-A receptor function and

dysfunction in AD and of ripple modulatory function as a possible prodromal biomarker for AD onset *in vivo*.

Declarations

Author contribution statement

David Howard Farb: Conceived and designed the experiments; Analyzed and interpreted the data; Wrote the paper.

R. Jonathan Robitsek: Conceived and designed the experiments; Performed the experiments; Analyzed and interpreted the data.

Marcia H. Ratner: Conceived and designed the experiments; Performed the experiments; Analyzed and interpreted the data; Wrote the paper.

Weiming Xia: Conceived and designed the experiments; Performed the experiments.

Tara M. Stewart, Vidhya Kumaresan, Ouyang Guo and KathrynAnn E. Odamah: Performed the experiments; Analyzed and interpreted the data.

Scott S. Downing: Analyzed and interpreted the data; Contributed reagents, materials, analysis tools or data; Wrote the paper.

Funding statement

David H Farb was supported by National Institute on Aging (R21AG056947, P01AG9973).

Marcia H. Ratner was supported by National Institute on Aging (T32AG00115).

Tara M. Stewart was supported by National Institute of Neurological Disorders and Stroke (F31NS068219) and National Institute of General Medical Sciences (T32GM008541).

Data availability statement

Data will be made available on request.

Declaration of interests statement

The authors declare no conflict of interest.

Additional information

Supplementary content related to this article has been published online at https://doi.org/10.1016/j.heliyon.2021.e07895. A preprint of a previous version of this research is availale at "Prodromal dysfunction of α5GABA-A receptor modulated hippocampal ripples in Alzheimer's disease" Ratner M.H. Downing S.S., Guo O., Odamah KE, Stewart T.M.,Kumaresan V., Robitsek R,J., Xia W, Farb D.H. bioRxiv 2021.05.10.443512; doi: https://doi.org/10.1101/2021.05.10.443512.

Acknowledgements

We dedicate this paper in memory of our collaborator Howard B. Eichenbaum, PhD, who was instrumental in helping us establish *in vivo* electrophysiology as a platform for advancing an understanding of memory through pharmacology. His scientific contributions to this research sadly ended prior to completion of the research. We also would like to thank Sam McKenzie, PhD, John Bladon, PhD, and Shelley J Russek, PhD for their many thoughtful and helpful comments and suggestions over the past two years. **Non-author Contributions:** The authors thank Dr. L. Adrienne Cupples for her assistance with statistical analysis and Dr. Yunlong Bai of the Harbin Medical University in China for his assistance with our validation of the offline ripple detection code used in these experiments. DHF thanks Michaela Gallagher (John's Hopkins) for her generous contributions toward helping us establish this line of investigation.

References

[1] S. McKenzie, H. Eichenbaum H, Consolidation and reconsolidation: two lives of memories? Neuron 71 (2011) 224–233.
[2] G. Buzsáki, Hippocampal sharp wave-ripple: a cognitive biomarker for episodic memory and planning, Hippocampus 25 (2015) 1073–1188.
[3] S.P. Jadhav, C. Kemere, P.W. German, L.M. Frank, Awake hippocampal sharp-wave ripples support spatial memory, Science 336 (2012) 1454–1458.
[4] I.A. Wilson, S. Ikonen, M. Gallagher, H. Eichenbaum, H. Tanila, Age-associated alterations of hippocampal place cells are subregion specific, J. Neurosci. 25 (2005) 6877–6886.
[5] M.A. Yassa, S.M. Stark, A. Bakker, M.S. Albert, M. Gallagher M, C.E. Stark, High-resolution structural and functional MRI of hippocampal CA3 and dentate gyrus in patients with amnestic Mild Cognitive Impairment, Neuroimage 51 (2010) 1242–1252.
[6] J. Robitsek, M.H. Ratner, T. Stewart, H. Eichenbaum, D.H. Farb, Combined administration of levetiracetam and valproic acid attenuates age-related hyperactivity of CA3 place cells, reduces place field area, and increases spatial information content in aged rat hippocampus, Hippocampus 25 (2015) 1541–1555.
[7] H. Lee, Z. Wang, S.L. Zeger, M. Gallagher, J.J. Knierim, Heterogeneity of age-related neural hyperactivity along the CA3 transverse Axis, J. Neurosci. 41 (2021) 663–673.
[8] J.J. Donegan, A.M. Boley, J. Yamaguchi, G.M. Toney, D.J. Lodge, Modulation of extrasynaptic GABAA alpha 5 receptors in the ventral hippocampus normalizes physiological and behavioral deficits in a circuit specific manner, Nat. Commun. 10 (2019) 2819.
[9] Z.M. Reagh, J.A. Noche, N.J. Tustison, D. Delisle, E.A. Murray, M.A. Yassa, Functional imbalance of anterolateral entorhinal cortex and hippocampal dentate/CA3 underlies age-related object pattern separation deficits, Neuron 97 (2018) 1187–1198.
[10] A. Branch, A. Monasterio, G. Blair, J.J. Knierim, M. Gallagher, R.P. Haberman, Aged rats with preserved memory dynamically recruit hippocampal inhibition in a local/global cue mismatch environment, Neurobiol. Aging 76 (2019) 151–161.
[11] A. Bakker, M.S. Albert, G. Krauss G, C.L. Speck, M. Gallagher, Response of the medial temporal lobe network in amnestic mild cognitive impairment to therapeutic intervention assessed by fMRI and memory task performance, Neuroimage Clin. 7 (2015) 688–698.
[12] M.T. Koh, S. Rosenzweig-Lipson, M. Gallagher M, Selective GABA(A) α5 positive allosteric modulators improve cognitive function in aged rats with memory impairment, Neuropharmacology 64 (2013) 145–152.
[13] G.R. Dawson, K.A. Maubach, N. Collinson, M. Cobain, B.J. Everitt, A.M. MacLeod, et al., An inverse agonist selective for alpha5 subunit-containing GABA-A receptors enhances cognition, J. Pharmacol. Exp. Therapeut. 316 (2006) 1335–1345.
[14] R.P. Bonin, L.J. Martin, J.F. MacDonald, B.A. Orser, Alpha5 GABA-A receptors regulate the intrinsic excitability of mouse hippocampal pyramidal neurons, J. Neurophysiol. 98 (2007) 2244–2254.
[15] J.R. Atack, W. Eng, R.E. Gibson, C. Ryan, B. Francis, B. Sohal, et al., The plasma-occupancy relationship of the novel GABA-A receptor benzodiazepine site ligand, alpha5IA, is similar in rats and primates, Br. J. Pharmacol. 157 (2009) 796–803.
[16] N. Collinson, J.R. Atack, P. Laughton, G.R. Dawson, D.N. Stephens, An inverse agonist selective for alpha5 subunit-containing GABA-A receptors improves encoding and recall but not consolidation in the Morris water maze, Psychopharmacology 188 (2006) 619–628.
[17] R. M Cohen, K. Rezai-Zadeh, T.M. Weitz, A. Rentsendorj, D. Gate, I. Spivak I, et al., A transgenic Alzheimer rat with plaques, tau pathology, behavioral impairment, oligomeric aβ, and frank neuronal loss, J. Neurosci. 33 (2013) 6245–6256.
[18] A. Hussin, T. Leonard, K. Hoffman, Sharp-wave ripple features in macaques depend on behavioral state and cell-type specific firing, Hippocampus 30 (2020) 50–59.
[19] V. Ego-Stengel, M.A. Wilson, Disruption of ripple-associated hippocampal activity during rest impairs spatial learning in the rat, Hippocampus 20 (2006) 1–10.
[20] A.K. Shetty, D.A. Turner, Hippocampal interneurons expressing glutamic acid decarboxylase and calcium-binding proteins decrease with aging in Fischer 344 rats, J. Comp. Neurol. 394 (1998) 252–269.
[21] K.D. Harris, D.A. Henze, J. Csicsvari, H. Hirase, G. Buzs√°ki, Accuracy of tetrode spike separation as determined by simultaneous intracellular and extracellular measurements, J. Neurophysiol. 84 (2000) 401–414.
[22] H. Tanila, M. Shapiro, M. Gallagher, H. Eichenbaum, Brain aging: changes in the nature of information coding by the hippocampus, J. Neurosci. 17 (1997) 5155–5166.
[23] R.W. Komorowski, J.R. Manns, H. Eichenbaum, Robust conjunctive item-place coding by hippocampal neurons parallels learning what happens where, J. Neurosci. 29 (2009) 9918–9929.
[24] C. Lever, T. Wills, F. Cacucci, N. Burgess, J. O'Keefe, Long-term plasticity in hippocampal place-cell representation of environmental geometry, Nature 416 (2002) 90–94.
[25] W.E. Skaggs, B.L. McNaughton, K.M. Gothard, E.J. Markus, An information-theoretic approach to deciphering the hippocampal code, in: Proceeding Advances in Neural Information Processing Systems 5 [NIPS conference], Morgan Kaufmann Publishers Inc, 1993, pp. 1030–1037.

[26] R. Fisher, Frequency distribution of the values of the correlation coefficient in samples from an indefinitely large population. Biometrika, 10 (4), pp. 507-521.
[27] N.T. Agnihotri, R.D. Hawkins, E.R. Kandel, C. Kentros, The long-term stability of new hippocampal place fields requires new protein synthesis, Proc. Natl. Acad. Sci. U. S. A. 101 (10) (2004 Mar 9) 3656–3661.
[28] J. Csicsvari, H. Hirase, A. Czurká, A. Mamiya, G. Buzsáki, Fast network oscillations in the hippocampal CA1 region of the behaving rat, J. Neurosci. 19 (16) (1999 Aug 15) RC20.
[29] J.F. Ramirez-Villegas, N.K. Logothetis, M. Besserve, Diversity of sharp-wave-ripple LFP signatures reveals differentiated brain-wide dynamical events, Proc. Natl. Acad. Sci. U. S. A. 112 (2015) E6379–E6387.
[30] A. Ennaceur, J. Delacour, A new one-trial test for neurobiological studies of memory in rats. 1: behavioral data, Behav. Brain Res. 31 (1988) 47–59.
[31] T. Murai, S. Okuda, T. Tanaka, H. Ohta, Characteristics of object location memory in mice: behavioral and pharmacological studies, Physiol. Behav. 90 (2007) 116–124.